

---

*Research Article: Open Source Tools and Methods | Novel Tools and Methods*

## **3D printable device for automated operant conditioning in the mouse**

<https://doi.org/10.1523/ENEURO.0502-19.2020>

**Cite as:** eNeuro 2020; 10.1523/ENEURO.0502-19.2020

Received: 31 March 2020

Revised: 21 January 2020

Accepted: 31 January 2020

---

*This Early Release article has been peer-reviewed and accepted, but has not been through the composition and copyediting processes. The final version may differ slightly in style or formatting and will contain links to any extended data.*

**Alerts:** Sign up at [www.eneuro.org/alerts](http://www.eneuro.org/alerts) to receive customized email alerts when the fully formatted version of this article is published.

Copyright © 2020 Mazziotti et al.

This is an open-access article distributed under the terms of the Creative Commons Attribution 4.0 International license, which permits unrestricted use, distribution and reproduction in any medium provided that the original work is properly attributed.

1 Manuscript Title:

2 **3D printable device for automated operant conditioning in the mouse**

3 Abbreviated Title :

4 **3D printable conditioning box for mice**

5

6 List of all Authors and Affiliations:

7 Raffaele Mazziotti<sup>1,2,\$</sup>, Giulia Sagona<sup>2,3,\$</sup>, Leonardo Lupori<sup>2,4</sup>, Virginia Martini<sup>2</sup>,  
8 Tommaso Pizzorusso<sup>1,2,4</sup>

9

10 *1. Department of Neuroscience, Psychology, Drug Research and Child Health*  
11 *NEUROFARBA University of Florence, Area San Salvi – Pad. 26, 50135 Florence,*  
12 *Italy*

13 *2. Institute of Neuroscience, National Research Council, Via Moruzzi, 1 56124*  
14 *Pisa, Italy*

15 *3. Department of Developmental Neuroscience, IRCCS Stella Maris Foundation,*  
16 *56128 Pisa, Italy*

17 *4. BIO@SNS lab, Scuola Normale Superiore via G. Moruzzi, 1 56124 Pisa, Italy*

18

19 *\$ These authors contributed equally to this work*

20 Authors' contributions:

21 R.M. designed behavioral apparatus, wrote the software and analyzed data. GS and  
22 V.M. performed experiments and analyzed data, L.L. contributed in the apparatus  
23 and software design. R.M., G.S., L.L., T.P. wrote the manuscript.

24 Correspondence should be addressed to:

25 *Raffaele Mazziotti, Istituto Neuroscienze CNR, Via G. Moruzzi, 1 56125 Pisa ITALY,*  
26 *tel +390503153167, Fax +390503153220 e-mail: [raffaele.mazziotti@in.cnr.it](mailto:raffaele.mazziotti@in.cnr.it)*

27 Number of Figures: 4

28 Number of Tables: 2

29 Number of Multimedia: 2

30 Number of words for Abstract: 178

31 Number of words for Significance Statement: 76

32 Number of words for Introduction: 328

33 Number of words for Discussion: 395

34 Acknowledgements:

35 We would like to thank the following people who kindly provided technical support:  
36 Sara Stefanini (for support with the exploded-view of the 3D model), Renzo di Renzo  
37 (for providing us resistors), Keagan Duneville (for critical revision of the work).

38 Conflict of Interest:

39 All authors declare no conflicts of interests.

40 Funding sources:

41 This work has been supported by Fondazione Telethon [GGP15098]; a research  
42 grant from the University of Pennsylvania Orphan Disease Center on behalf of  
43 LouLou Foundation and in partnership with The International Foundation for CDKL5  
44 Research.

45

## 46 Abstract

47

48

49 Operant conditioning is a classical paradigm and a standard technique used in experimental  
50 psychology in which animals learn to perform an action in order to achieve a reward. By  
51 using this paradigm, it is possible to extract learning curves and measure accurately reaction  
52 times. Both these measurements are proxy of cognitive capabilities and can be used to  
53 evaluate the effectiveness of therapeutic interventions in mouse models of disease. Here we  
54 describe a fully 3D printable device that is able to perform operant conditioning on freely  
55 moving mice, while performing real-time tracking of the animal position. We successfully  
56 trained 6 mice, showing stereotyped learning curves that are highly reproducible across  
57 mice and reaching more than 70% of accuracy after two days of conditioning. Different  
58 products for operant conditioning are commercially available, though most of them do not  
59 provide customizable features and are relatively expensive. This data demonstrate that this  
60 system is a valuable alternative to available state-of-the-art commercial devices,  
61 representing a good balance between performance, cost, and versatility in its use.  
62

## 63 Significance Statement

64 3D printing is a revolutionary technology that combines cost-effectiveness with an optimal  
65 trade off between standardization and customization. Here we show a device that performs  
66 operant conditioning in mice using largely 3D printed parts. This tool can be employed to test  
67 learning and memory in models of disease. We expect that the open design of the chamber  
68 will be useful for scientific teaching and research as well as for further improvements from  
69 the open hardware community.  
70

71

72

73

## 74 Introduction

75 Operant conditioning (OC) (Jones, Nowell Jones, and Skinner 1939) is a standard technique  
76 used in experimental psychology in which animals, like rodents (Francis and Kanold 2017;  
77 O'Leary et al. 2018), reptiles (Mueller-Paul et al. 2014), birds (Cook 1992), dogs (Range et  
78 al. 2008), monkeys (Range et al. 2008), and humans (Angulo-Barroso et al. 2017; Siqueland  
79 1964), learn to perform an action in order to achieve a reward. By using this paradigm, it is  
80 possible to extract learning curves and measure accurately mental chronometry (e.g.  
81 reaction times). As previously suggested (Escobar and Pérez-Herrera 2015; O'Leary et al.  
82 2018; Francis and Kanold 2017), different products for OC are commercially available,  
83 though most of them do not provide customizable features and are relatively expensive.

84 Neuroscience research has greatly benefited from new 3D printing technologies bringing  
85 new possibilities to build tools, and increasing productivity and user-timeliness. 3D printing  
86 also opened unprecedented resources for training students and solving common  
87 experimental problems (Baden et al. 2015). There is a plethora of work using 3D printed  
88 mechanical parts (Baden et al. 2015), ranging from fluorescence microscopes (Chagas et al.  
89 2017) to electrophysiology systems (Siegle et al. 2017). The combination of 3D printing with  
90 off-the-shelf, low-cost optical and electronic components facilitates reproducibility of  
91 experimental tools internationally and promotes rapid iteration and prototyping (Chagas et al.  
92 2017). Here we demonstrate an affordable, fully 3D printable, and automated solution that  
93 can be reproduced rigorously in any laboratory equipped with a 3D printer with a total cost  
94 around 160€ (Table 1). We designed the chamber entirely using 3D modelling for several  
95 reasons: first, it has a high degree of reproducibility, since the model is standardized and can  
96 be downloaded to print the same structure with the same materials throughout different  
97 laboratories. Secondly, it can be easily customized in relation with specific experimental  
98 needs. Lastly, it can be easily shared through on-line repositories. With these cost-efficient  
99 and accessible components, we assayed the possibility to perform two-alternative forced  
100 choice operant conditioning using audio-visual cues while tracking in real time mouse  
101 position.  
102

## 103 **Methods**

### 104 **Mice housing and handling**

105 Animals were kept at a constant temperature (22°C) with a standard 12h light-dark cycle  
106 (7am to 7 pm). Food was available ad libitum and changed weekly. During OC Protocol mice  
107 are water restricted (body weight > 85% (Goltstein et al. 2018)) of their baseline. Before the  
108 experiment mice are handled for 1 hour/day for 1 week. After the last daily session, mice  
109 had free access to water for 1 hour (23 hours of water deprivation). All the experiments  
110 were carried out in accordance with the directives of European Community Council  
111 (2011/63/EU) and approved by the Italian Ministry of Health. We tested 6 wild-type  
112 C57BL/6J (from P50 to P180, 4 female and 2 male mice, Charles River).  
113  
114

### 115 **3D printed operant conditioning chamber**

116 The OC arena (16x16x16 cm, thickness 3 mm, Fig.1.a) is 3D printed using gray or white  
117 PLA (B06W568X1G, Technology Outlet). The 3D project is designed using FreeCAD  
118 software, exported in stereolithography (STL) format, converted to G-code using Cura  
119 (<https://ultimaker.com/software/ultimaker-cura>) and printed using Kentstrapper Verve 3D  
120 printer (<https://kentstrapper.com/stampante-3d-kentstrapper-verve/>). In Fig.1.c an exploded-  
121 view drawing of the chamber is shown. The color coding corresponds to different  
122 components of the apparatus (visual stimulation parts in red; camera holder in green;  
123 syringe pump in purple). All these components are coated using epoxy transparent resin  
124 (LF-L2GR-26GX, resinpro), that allows cleaning (5% ethanol in water). The arena front wall  
125 contains the elements interfacing the animal with the computer. It can be modularly

126 assembled to the arena and is composed by a squared frame containing the LED matrix at  
127 the center, four holes for the touch buttons in the lower part, a central hole for the lick spout  
128 and a hole in the upper part to connect a piezo buzzer. The touch buttons are printed using  
129 graphene PLA (PLA\_GRAFENE\_175, filoprint), and connected using conductive glue  
130 (Chemtronics: CW2400) to a female pin (B07XQHD752, amazon.it) using a resistor (25  
131 MOhm). A dotted grid is interposed between the LED matrix and the inside of the chamber  
132 and has two roles: first, the dotted pattern restricts the visibility of the LED lights to equal  
133 small circles; second, it contains a grid of walls facing the LEDs that prevents the light from  
134 each source to spill over to the neighbouring dots. The LED matrix is covered with a thin  
135 white plexiglass foil, so that single LED are not visible if they are off and to diffuse light  
136 uniformly. The camera holder, is joint assembled on top of the frontal wall and it is designed  
137 to maintain the camera at the distance necessary to image the entire arena using a 3.6 mm  
138 focal length objective. The syringe pump is composed of a base that fixes the barrel of the  
139 syringe into position and of a piston that slides on a stepper motor guided M8 metal screw  
140 and allows to push or pull the plunger.

## 141 Hardware

142 An electronic board is mounted on a grounded metal sheet and is composed by a Raspberry  
143 Pi connected via USB to an Arduino UNO (AU) board ([https://store.arduino.cc/arduino-uno-](https://store.arduino.cc/arduino-uno-rev3)  
144 [rev3](https://store.arduino.cc/arduino-uno-rev3) ). The Raspberry Pi (<https://www.raspberrypi.org/products/raspberry-pi-3-model-b/> )  
145 acts as the main computer of the setup. It executes the Python 3 script that handles the  
146 structure of the experiment, performs computer vision using a Raspberry Pi camera  
147 (Bewinner: Bewinnertyv48w6mf5), and saves data (Fig.1.b). The AU controls sensors and  
148 actuators in the OC chamber. Two touch buttons, made using conductive PLA, acts as  
149 capacitive sensors and are connected to AU using coaxial cables (3mm diameter) to  
150 minimize environmental noise. The main advantage of using graphene PLA resides in the  
151 possibility to print different button designs (e.g. for motor impairment, nose poking, etc.).  
152 There are three actuators: a LED matrix serves as display (Adafruit: 1487), a piezo buzzer  
153 (Adafruit: PS1240, frequency range: 2-10kHz, 60 dB) is used as acoustic stimulator glued at  
154 the top of the frontal door, and a stepper motor (amazon.it: 28BYJ-48, with ULN2003)  
155 connected to a M8 screw guiding the piston of a syringe pump controlling a disposable  
156 syringe (10ml) connected with a silicone tube equipped by luer tapers adapters to a blunt  
157 needle (Warner instruments: SN-18) for reward delivery. This modular configuration allows  
158 the proper cleaning of the delivery tubing after each session. We use an external 5V 2A DC  
159 power supply (Samsung: TA10EWE) with a 1000 $\mu$ F capacitor to power the LED matrix and  
160 the stepper motor. A diagram of the electrical wiring is shown in the Fig.1.d.

## 161 Software

### 162 AU Program

163 The code controlling the OC box is organized in four files, the file called *skinner.ino* contains  
164 the logic of the experiment and manages the serial communication with the computer.  
165 Different files are dedicated to different aspects of the program: the file called *button.ino*  
166 contains functions to control the touch buttons and play auditory stimuli, the file called  
167 *ledLib.ino* contains wrapper functions to control Adafruit NeoPixel library  
168 (<https://www.adafruit.com/product/1487> ) and generate simple visual stimuli easily, the third

169 file called *stepper.ino*, contains functions to control the syringe pump using the Arduino  
170 Stepper motor library (<https://www.arduino.cc/en/reference/stepper> ). In summary, to setup  
171 the AU, a user needs to download the folder containing the *.ino* files, uncompress and  
172 upload the file *skinner.ino*.

### 173 Raspberry Pi program

174 On the Raspberry Pi, a Python script controlling the experiment has been written using IDLE.  
175 The program relies on a number of external libraries that are required to run all parts of the  
176 script with no errors. Since the task relies on real time tracking of the animal position we use  
177 *picamera* and *opencv* libraries to acquire frames and process them using K-nearest  
178 neighbours based Background-Foreground Segmentation (Zivkovic and van der Heijden  
179 2006), a widely used algorithm for generating a foreground mask using static cameras  
180 (Fig.2.a). The technique consists of two main steps, the first one is the background  
181 initialization in which we use 1000 frames of the empty arena, then we set the learning rate  
182 to zero and the algorithm stops updating the background so it's ready to locate reliably the  
183 position of the animal with a frame rate of 20 Hz. *LibSerial* library is used to communicate  
184 with the AU during the task sending symbolic codes and changing the state of the AU in the  
185 OC chamber. We used *Tkinter* library to write the initial GUI to set the experimental  
186 parameters. The behavioral sequence is outlined in Fig.2.b. Virtually the chamber can be  
187 divided into two sections: the anterior part that contains the interface between the mouse  
188 and the computer, and the posterior side that is designed as an *active area* to activate the  
189 trials. If the mouse remains in the *active area* for a given amount of time (1.5 seconds) the  
190 trial is triggered. At this stage a visual stimulus is shown on the display and the system waits  
191 for animal response. When the mouse touches one of the two buttons, an auditory feedback  
192 is produced, with a tone that varies depending on whether the answer is correct (3300 Hz) or  
193 wrong (2700 Hz). In case of correct answer a drop (7  $\mu$ L) of water with 1% condensed milk is  
194 released.  
195

### 196 Implementation of an LCD screen

197 As a proof of principle of customizability, we added a version of the OC chamber that is able  
198 to show more complex visual stimuli. This version includes an edit of the frontal wall that  
199 can host a TFT monitor (Kookye 3.5" for RPI3) and a folder (LCD\_oc\_chamber) containing  
200 code that runs on Psychopy2 (Peirce 2008), a Python package dedicated to behavioral  
201 experiments. This configuration allows to show RGB images as visual stimuli (Movie 2).  
202

### 203 Code Accessibility

204 The code described in the paper is freely available online at  
205 [https://github.com/raffaelemazziotti/oc\\_chamber](https://github.com/raffaelemazziotti/oc_chamber) . The code is also available as Extended  
206 Data 1.  
207

### 208 The OC protocol

209 *Familiarization*. This phase is carried out by placing each animal in the OC box for 3  
210 sessions of 10 minutes, spaced by at least 2 hours between each other. During this phase, a



211 liquid reward, coupled with the “correct” tone is provided manually whenever the mouse is in  
212 the active area, in this way the animal learns where to find the reward and associate it with  
213 the tone.

214 *Shaping* (3 days). The visual stimulus is introduced (Fig.2.c). It consists of two bright (0.9  
215  $\text{cd/m}^2$ ) blue (465-475nm) dots (5mm) that appear above the two buttons. The mouse needs  
216 to touch one of the two buttons to obtain the reward.

217 *Operant task (OT, 5 days)*. During this phase, only one dot appears, identifying the correct  
218 button. If the mouse touches the correct button, the “correct” tone is reproduced and the  
219 animal receives the reward. If the mouse touches the wrong button, the “wrong” tone is  
220 reproduced and no liquid reward will be delivered. This procedure is shown in Fig.2.c. The  
221 sequence of stimuli is balanced so that the mouse sees each case the same number of  
222 times. In order to prevent perseveration with the same answer, during the first 2 days we  
223 adopted an assisted procedure (Fig.2.d): the first stimulus presented is random, if the mouse  
224 produces the correct answer the following stimulus is randomized, in case of wrong answer  
225 instead, the system repeats the same stimulus until the mouse gives the correct answer 3  
226 times.

227 *Follow-ups*. In order to test the ability of the mouse to recall the task we tested animals in  
228 different follow-ups, respectively at 6 days, 27 days, 3 months and 4 months approximately  
229 after the end of OT. For each recall sessions we tested mice once per day.

## 230 Data analysis and statistics

231 Data processing is performed using Python and the statistical analysis (Table 2) using  
232 GraphPad Prism 7. To analyze mouse tracking data the arena is virtually divided into 256  
233 (16x16) bins and raw exploration is z-scored to obtain relative exploration measures. To  
234 quantitatively test if the mouse preferentially explores some of the bins, we constructed a  
235 resampled binned exploration matrix representing chance level for each bin, randomly  
236 permuting each animal exploration matrix for 100 times. The software Fritzing was used  
237 to draw the wiring diagram of the electrical components. We used Rhino 6 to draw the  
238 exploded version of the model.

239

## 240 Results

### 241 Behavioral Performance

242 To test our system ability to detect learning curves we trained mice as depicted in the  
243 protocol in Fig.3b. Table 2 reports all statistical analysis. In shaping phase, the average  
244 number of trials (TR) progressively increases over time for all the subjects and specifically  
245 the third day, we detect a significant increase compared to the first day. Moreover, reaction  
246 times (RT) and intertrial Intervals (ITI) showed a similar trend with a significant reduction of  
247 the RT starting from the second day (Fig.3a). This indicates that already at Day 2 the animals  
248 started to refine the sequence of actions necessary to trigger the stimulus and produce a  
249 response. Next, the results of the OT phase are shown in Fig.3c. The average TR continued  
250 to grow until day Day 3 of OT. After this day, the majority of the animals performed the  
251 maximum TR permitted in each session. Both RT and ITI showed a decrease with time.  
252 Indeed, RT and ITI dropped significantly during the first two days and reached a plateau by

253 the third day. We observed a significant difference in the percentage of correct responses  
254 between the first and second day. In order to assess the retention of the test over time, we  
255 tested the same mice at different time points after the end of the OT. Accuracy remained  
256 stable during all time points tested, however RT showed a more complex pattern: with an  
257 initial decrease, compared to the last day of the OT, followed by an increase at 4 months.  
258 Analyzing ITI, we detected an increase of the time between two trials at 27 days that  
259 remained higher at 3 and 4 months compared to the end of the OT (Fig.3d). It is interesting  
260 to note that, since touch sensors are activated from all sides, some of the variability in timing  
261 performance could be explained by the development of different strategies to activate  
262 sensors.

263

### 264 Tracking Analysis

265 In Fig.4.a tracking traces, of all the mice, are shown with corresponding heatmaps, averaged  
266 across animals (on the right) or days (bottom row), showing non-uniform exploration of the  
267 OC chamber during tasks. Pixels that were not significantly explored compared to randomly  
268 resampled uniform exploration values ( $P$ -values $>0.05$ ) were set to 0. The reward area was  
269 the most visited place, as shown by both the animals and session average heatmaps. In the  
270 bottom half of the arena there are two significant exploration spots at the corners, that  
271 indicate a stereotyped strategy to activate the trial (Fig.4.b). Moreover, we analysed the  
272 distance travelled by each animal inside the OC box during all the tasks. We found that,  
273 throughout the course of the shaping phase, there was a significant decrease in the total  
274 amount of distance travelled compared to the first day (Fig.4). Conversely, during the OT  
275 phase, we detected no changes ( $p=0.3672$ ). Interestingly, we found a significant correlation  
276 between timing performances and the total distance moved during shaping (Fig.4.c), this  
277 suggests that about 25% ( $r^2=0.247$ ) of the improvement in timing performance is explained  
278 by a reduction in the distance travelled and the response of the animal. In addition, no  
279 differences in the average speed were detectable during both shaping and OT. These  
280 results imply that the reduction of the RT is due to the optimization of the psychomotor  
281 sequence in realizing the task rather than to a general increase of velocity of the animal.

282

## 283 Discussion

284

285 Here we described a fully 3D printable device that performs operant conditioning on freely  
286 moving mice while tracking the animal position in real time. We successfully trained 6  
287 subjects, showing stereotyped learning curves that are highly reproducible across mice and  
288 reaching more than 70% of accuracy after two days of conditioning (Movie 1). This dataset  
289 demonstrate that this system is a valuable low cost alternative to available state-of-the-art  
290 commercial devices, representing a good balance between performance, cost, and  
291 versatility. Performances detected by our system in three sessions per day ( $3.97\pm 0.11$   
292 trial/min with an accuracy of  $84.1\pm 1.7\%$ ) are comparable with normative values detected in  
293 C57BL/6J and measured on an analogous 2 alternative forced choice task performed once  
294 daily (Malkki et al. 2010). Although the LED display does not allow to design complex visual  
295 patterns required to perform image recognition and classification, visual stimulation is flexible



296 enough to design simple tasks to test attention, learning, memory and other  
297 neuropsychological aspects of cognition (Escobar and Pérez-Herrera 2015; D'Ausilio 2012).  
298 The system is also easily customizable, as it is possible to add a LCD display guided by  
299 extra Python libraries (e.g. Pygame or Psychopy). The overall cost of the chamber is around  
300 160€, but can be further substantially reduced using cheaper boards compared to AU and a  
301 Raspberry Pi. There are other low-cost alternatives for operant conditioning (Francis and  
302 Kanold 2017; Escobar and Pérez-Herrera 2015; O'Leary et al. 2018), however, the main  
303 strength of the present device is the high degree of reproducibility, since the model is  
304 standardized and can be downloaded to print the same structure with the same materials  
305 throughout different laboratories. Secondly, it can be customized in relation with specific  
306 experimental needs (e.g. very young animals). Lastly, different versions of the OC chamber  
307 can be tested and shared through on-line repositories, such as Thingiverse  
308 (<https://www.thingiverse.com/>) and NIH Print Exchange (<https://3dprint.nih.gov/>). Moreover,  
309 the OC chamber includes real time tracking of the mouse position, a feature that could be  
310 used as second phenotyping measure of anxiety or stereotyped behaviors. Additionally it  
311 allows to analyse other aspects of behavior, such as inhibitory control (Munakata et al.  
312 2011). For example, by increasing the time required to trigger a trial, it is possible to  
313 measure impulsivity or reproduce neuropsychological tests used on humans like delayed  
314 gratification or stop signal tasks (Pinkston and Lamb 2011; Furlong et al. 2016). It is also  
315 plausible to couple the procedure with physiological recordings in freely moving conditions  
316 such as imaging techniques (e.g. fiber photometry) and electrophysiology. Thanks to the  
317 general-purpose input/output ports (GPIO) of both AU and Raspberry Pi boards, high  
318 precision synchronization of physiological recordings with behavioural events is accurately  
319 integrated within experimental recording paradigms. The simplicity and modularity of the  
320 apparatus can be exploited as an educational tool to train students in 3D printing and coding.  
321 For these reasons, we expect that the open design of the OC chamber will be useful for  
322 teaching and research as well as for further design improvements from the international  
323 open hardware community.

## 324 References

325  
326

- 327 Angulo-Barroso, Rosa M., Susana Pecifia, Xu Lin, Mingyan Li, Julia Sturza, Jie Shao, and  
328 Betsy Lozoff. 2017. "Implicit Learning and Emotional Responses in Nine-Month-Old  
329 Infants." *Cognition & Emotion* 31 (5): 1031–40.
- 330 Baden, Tom, Andre Maia Chagas, Gregory J. Gage, Timothy C. Marzullo, Lucia L. Prieto-  
331 Godino, and Thomas Euler. 2015. "Open Labware: 3-D Printing Your Own Lab  
332 Equipment." *PLoS Biology* 13 (3): e1002086.
- 333 Chagas, Andre Maia, Lucia L. Prieto-Godino, Aristides B. Arrenberg, and Tom Baden. 2017.  
334 "The €100 Lab: A 3D-Printable Open-Source Platform for Fluorescence Microscopy,  
335 Optogenetics, and Accurate Temperature Control during Behaviour of Zebrafish,  
336 Drosophila, and Caenorhabditis Elegans." *PLOS Biology*.  
337 <https://doi.org/10.1371/journal.pbio.2002702>.
- 338 Cook, Robert G. 1992. "Acquisition and Transfer of Visual Texture Discriminations by  
339 Pigeons." *Journal of Experimental Psychology: Animal Behavior Processes*.  
340 <https://doi.org/10.1037/0097-7403.18.4.341>.
- 341 D'Ausilio, Alessandro. 2012. "Arduino: A Low-Cost Multipurpose Lab Equipment." *Behavior*

- 342 *Research Methods*. <https://doi.org/10.3758/s13428-011-0163-z>.
- 343 Escobar, Rogelio, and Carlos A. Pérez-Herrera. 2015. "Low-Cost USB Interface for Operant  
344 Research Using Arduino and Visual Basic." *Journal of the Experimental Analysis of*  
345 *Behavior* 103 (2): 427–35.
- 346 Francis, Nikolas A., and Patrick O. Kanold. 2017. "Automated Operant Conditioning in the  
347 Mouse Home Cage." *Frontiers in Neural Circuits* 11 (March): 10.
- 348 Furlong, Teri M., Lee S. Leavitt, Kristen A. Keefe, and Jong-Hyun Son. 2016.  
349 "Methamphetamine-, D-Amphetamine-, and P-Chloroamphetamine-Induced  
350 Neurotoxicity Differentially Effect Impulsive Responding on the Stop-Signal Task in  
351 Rats." *Neurotoxicity Research* 29 (4): 569–82.
- 352 Goltstein, Pieter M., Sandra Reinert, Annet Glas, Tobias Bonhoeffer, and Mark Hübener.  
353 2018. "Food and Water Restriction Lead to Differential Learning Behaviors in a Head-  
354 Fixed Two-Choice Visual Discrimination Task for Mice." *PLoS One* 13 (9): e0204066.
- 355 Jones, F. Nowell, F. Nowell Jones, and B. F. Skinner. 1939. "The Behavior of Organisms: An  
356 Experimental Analysis." *The American Journal of Psychology*.  
357 <https://doi.org/10.2307/1416495>.
- 358 Malkki, Hemi A. I., Laura A. B. Donga, Sabine E. de Groot, Francesco P. Battaglia,  
359 NeuroBSIK Mouse Phenomics Consortium, and Cyriel M. A. Pennartz. 2010. "Appetitive  
360 Operant Conditioning in Mice: Heritability and Dissociability of Training Stages."  
361 *Frontiers in Behavioral Neuroscience* 4 (November): 171.
- 362 Mueller-Paul, Julia, Anna Wilkinson, Ulrike Aust, Michael Steurer, Geoffrey Hall, and Ludwig  
363 Huber. 2014. "Touchscreen Performance and Knowledge Transfer in the Red-Footed  
364 Tortoise (*Chelonoidis Carbonaria*)." *Behavioural Processes* 106 (July): 187–92.
- 365 Munakata, Yuko, Seth A. Herd, Christopher H. Chatham, Brendan E. Depue, Marie T.  
366 Banich, and Randall C. O'Reilly. 2011. "A Unified Framework for Inhibitory Control."  
367 *Trends in Cognitive Sciences* 15 (10): 453–59.
- 368 O'Leary, James D., Olivia F. O'Leary, John F. Cryan, and Yvonne M. Nolan. 2018. "A Low-  
369 Cost Touchscreen Operant Chamber Using a Raspberry Pi™." *Behavior Research*  
370 *Methods* 50 (6): 2523–30.
- 371 Peirce, Jonathan W. 2008. "Generating Stimuli for Neuroscience Using PsychoPy." *Frontiers*  
372 *in Neuroinformatics* 2: 10.
- 373 Pinkston, Jonathan W., and R. J. Lamb. 2011. "Delay Discounting in C57BL/6J and DBA/2J  
374 Mice: Adolescent-Limited and Life-Persistent Patterns of Impulsivity." *Behavioral*  
375 *Neuroscience* 125 (2): 194–201.
- 376 Range, Friederike, Ulrike Aust, Michael Steurer, and Ludwig Huber. 2008. "Visual  
377 Categorization of Natural Stimuli by Domestic Dogs." *Animal Cognition* 11 (2): 339–47.
- 378 Siegle, Joshua H., Aarón Cuevas López, Yogi A. Patel, Kirill Abramov, Shay Ohayon, and  
379 Jakob Voigts. 2017. "Open Ephys: An Open-Source, Plugin-Based Platform for  
380 Multichannel Electrophysiology." *Journal of Neural Engineering* 14 (4): 045003.
- 381 Siqueland, Einar R. 1964. "Operant Conditioning of Head Turning in Four-Month Infants."  
382 *Psychonomic Science*. <https://doi.org/10.3758/bf03342878>.
- 383 Zivkovic, Zoran, and Ferdinand van der Heijden. 2006. "Efficient Adaptive Density Estimation  
384 per Image Pixel for the Task of Background Subtraction." *Pattern Recognition Letters*.  
385 <https://doi.org/10.1016/j.patrec.2005.11.005>.

386  
387

## 388 Captions

389  
390

Fig\_1

391 3D printable operant conditioning apparatus. A: Left: Top-view of the apparatus. Center:  
 392 interface wall. Right: blue dotted stimuli, camera holder and syringe pump. B: An animal  
 393 during the task, the blue line delimitates the “active zone” C: An exploded view of the project  
 394 showing the assembling scheme. D: Circuit diagram of all the components.

395

396 Fig\_2

397 Behavioral procedures. A: The detection of the mouse is obtained using background  
 398 subtraction from the current frame and then applying a threshold, isolating only the mouse  
 399 silhouette. B: Behavioral sequence to obtain the reward. C: Diagram showing the behavioral  
 400 procedures: during the shaping phase and the operating task. D: Flowchart of the assisted  
 401 procedure.

402

403 Fig\_3

404 Behavioral performance. A: Performance of the shaping phase. B: Operant conditioning  
 405 protocol. C: Performance during the OT. D: Performance during recall.

406

407 Fig\_4:

408 Tracking analysis. A: Matrix of tracking traces of all animals per all days, with marginal  
 409 heatmaps, showing spots of exploration significantly different from chance. Average  
 410 heatmaps per each animal and per each day are presented in the last column and in the last  
 411 row respectively. B: Relative exploration in the arena: reward area is the most frequently  
 412 explored followed by corners of the active area and the central spot. C: Correlation analysis  
 413 between performance and spatial tracking. D: Velocity and distance traveled during the  
 414 shaping phase and the OT.

415

## 416 Tables

417 Table 1

418 Bill of materials

419

MATERIAL	PRICE €	VENDOR	CODE	MANUFACTURER
LED MATRIX	26.74	<a href="https://www.amazon.it">amazon.it</a>	B071VJL91V	Kuman:WS01
stepper motor	3.38	<a href="https://www.amazon.it">amazon.it</a>	B00DGNO6PI	Elegoo
PLA	16.66	<a href="https://www.amazon.it">amazon.it</a>	B06W568X1G	TECHNOLOGY OUTLET
Pi camera	18.99	<a href="https://www.amazon.it">amazon.it</a>	B07P8PG5MF	Bewinner: Bewinnertyv48w6mf5
Raspberry PI	44.51	<a href="https://www.amazon.it">amazon.it</a>	B01CD5VC92	raspberrypi
Graphene PLA	27.50	<a href="https://www.filoprint.it">filoprint.it</a>	PLA_GRAFENE_175	Haydale
Arduino UNO	16.85	<a href="https://www.amazon.it">amazon.it</a>	B07SL2W4CL	Arduino: A000066

420  
421  
422  
423  
424

power supply	5.69	<a href="https://www.amazon.it">amazon.it</a>	B00UVOHJ0Y	Samsung:TA10EWE
Piezo Buzzer	1.35	<a href="https://www.adafruit.com">adafruit.com</a>	PS1240	tdk
cables/wires	2.00	off the shelf		
TOTAL	163.67			

Table 2  
Statistical table

Figure	Type of test	Statistical data
Fig 3A_Average trials	RM One-way ANOVA, Dunnett's multiple comparisons post hoc	p=0.0006, post hoc Day 1 vs Day 3, p<0.001
Fig 3A_RT	as above	p=0.0002, Day 1 vs Day 2, p=0.001 and Day 1 vs Day 3, p=0.0002
Fig 3A_ITI	as above	p=0.0002, Day 1 vs Day 2, p=0.0148 and Day 1 vs Day 3, p=0.0001
Fig 3C_Average trials	as above	p=0.0046, Day 1 vs Day 3, p=0.0057; Day 1 vs Day 4, p=0.0057 and Day 1 vs Day 5, p=0.0036
Fig 3C_RT	as above	p=0.0022, Day 1 vs Day 3, p=0.0027; Day 1 vs Day 4, p=0.0011 and Day 1 vs Day 5, p=0.0275
Fig 3C_ITI	as above	p<0.0001, Day 1 vs Day 3, p=0.0004; Day 1 vs Day 4, p<0.0001 and Day 1 vs Day 5, p=0.0002
Fig 3C_Correct	as above	p = 0.0025; Day 1 vs Day 2, p = 0.0464; Day 1 vs Day 3, p = 0.0043; Day 1 vs Day 4, p = 0.0042 and Day 1 vs Day 5, p = 0.0013;
Fig 3D_Average Trials	as above	p=0.0058; Baseline vs 4 months, p=0.0042
Fig 3D_RT	as above	p<0.0001, Baseline vs 6 days, p=0.0063; Baseline vs 4 months p<0.0001
Fig 3D_ITI	as above	p<0.0001, baseline vs 27 days, p=0.0093, baseline vs 3 months, p=0.0009, baseline vs 4 months, p=0.0252
Fig 3D_Correct	as above	p=0.2290

Fig 4B_Relative_exploration	as above	p<0.0001, Corner vs. Center, p<0.0001; Corner vs. Reward, p<0.0001, Center vs. Reward, p<0.0001
Fig 4C_Correlation_matrix_TR vs RT	Spearman Correlation(SC)	r=-0.8223 (95% CI -0.9335 to -0.5669); R2=0.6761
Fig 4C_Correlation_matrix_TR vs ITI	SC	r =-0.9472 (95% CI -0.9811 to -0.8573); R2=0.8971
Fig 4C_Correlation_matrix_ITI vs RT	SC	r=0.9209 (95% CI 0.7910 to 0.9714); R2 = 0.8480
Fig 4C_Correlation_matrix_DIST vs RT	SC	r=0.5666 (95% CI 0.1208 to 0.8222); R2=0.3210
Fig 4C_Correlation_matrix_DIST vs ITI	SC	r=0.4972 (95% CI 0.02450 to 0.7882); R2=0.2472
Fig 4D_Tracking_distance	One-way ANOVA, Holm-Sidak's post hoc	p=0.03; Day 1 vs Day 3, p=0.02

425

426 **Multimedia**

427 Movie 1

428 A movie of a session with 30 trials during OT.

429

430 Movie 2

431 A proof of principle of LCD screen functioning inside the OC box, under the same  
432 light conditions of stimulation.

433

434 Extended Data 1

435 Extended Data 1.zip contains the code for both Arduino and Raspberry Pi boards

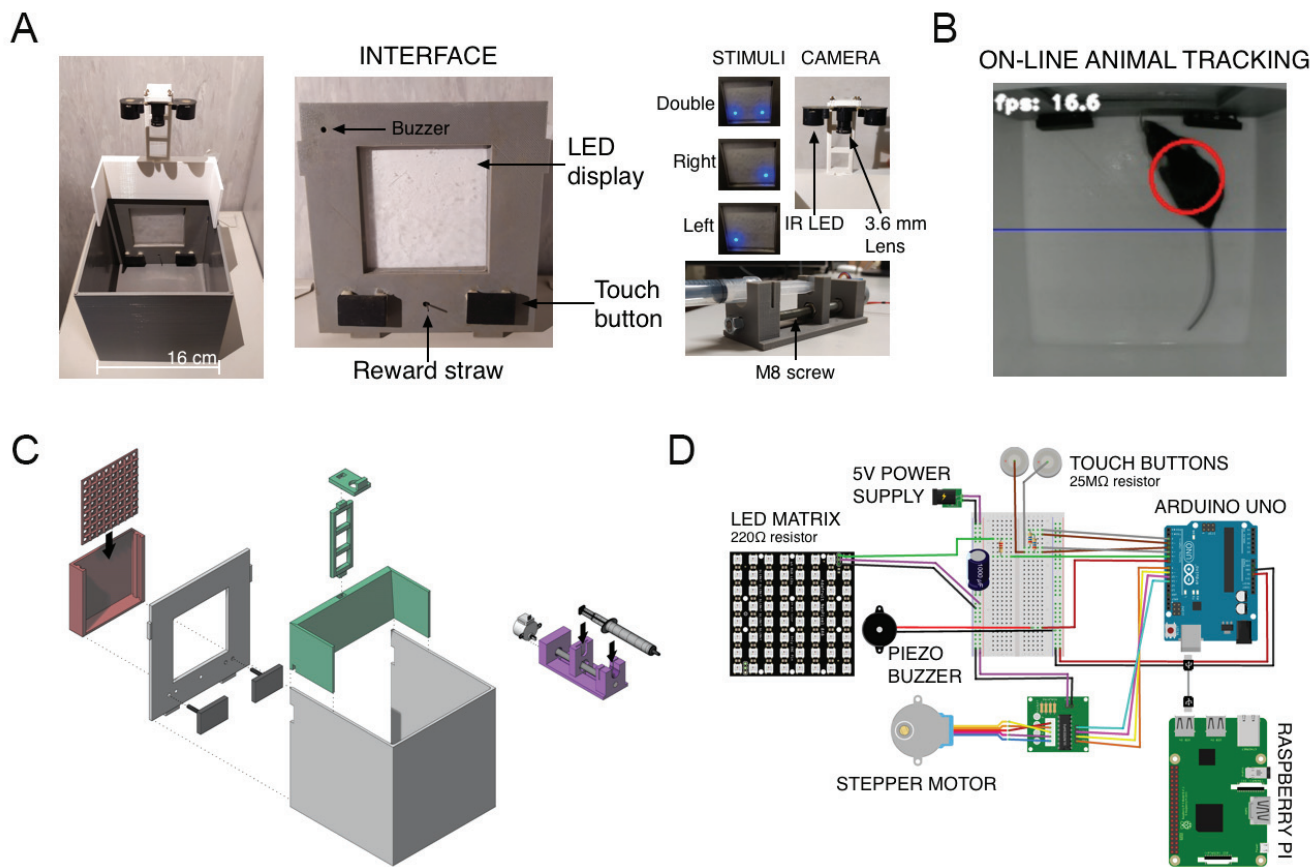
436

437

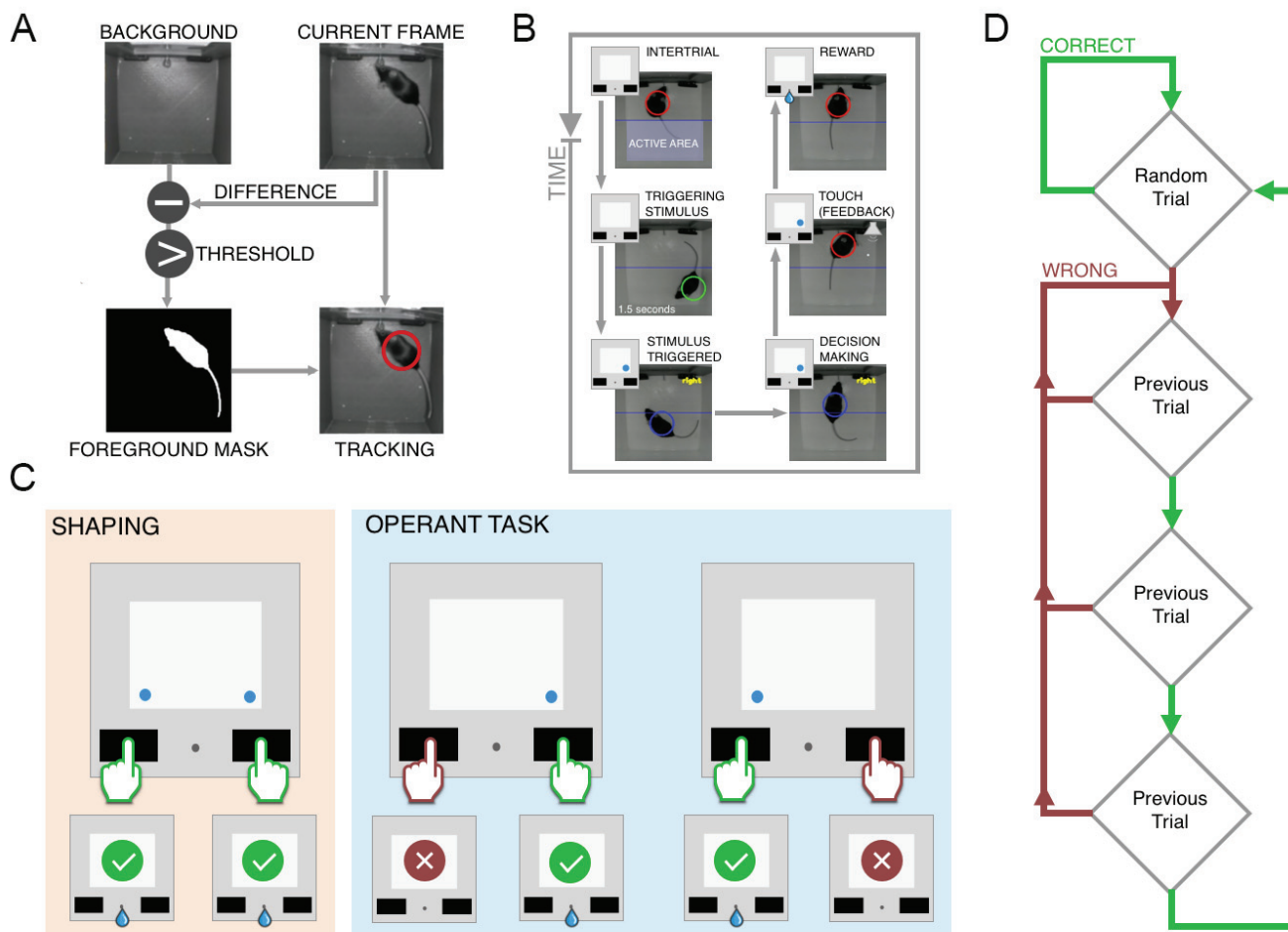
438

439

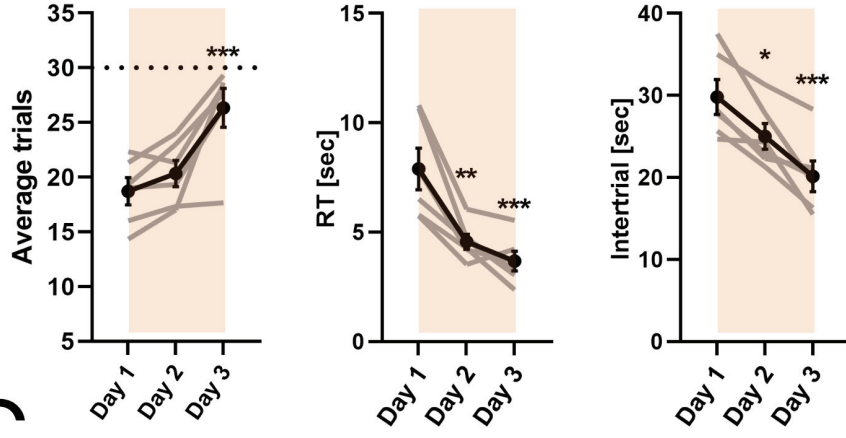
440



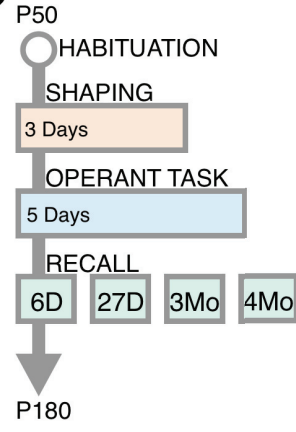




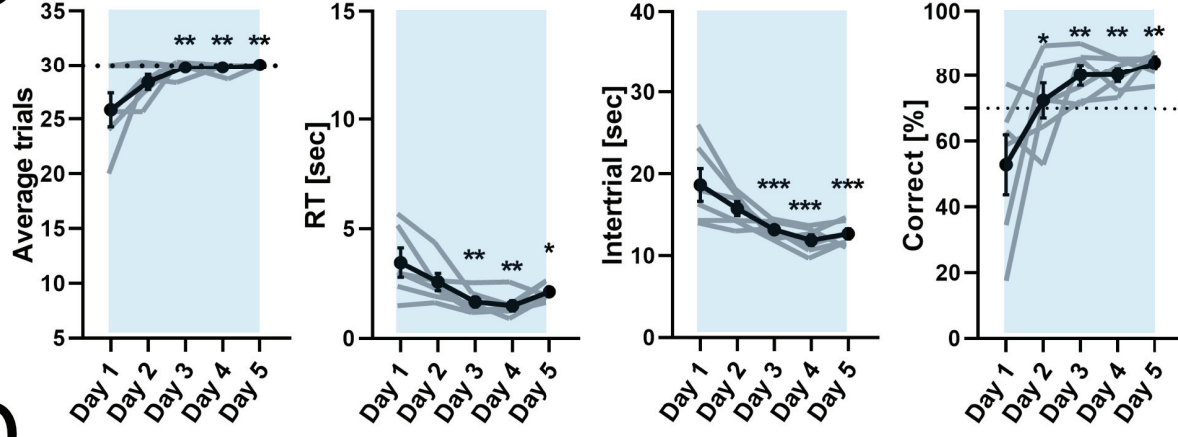
**A**



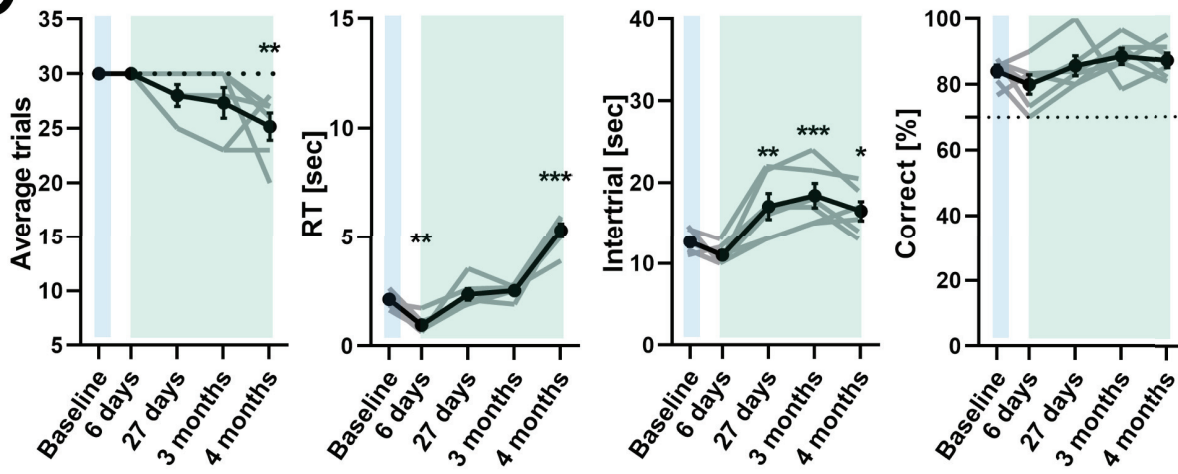
**B**



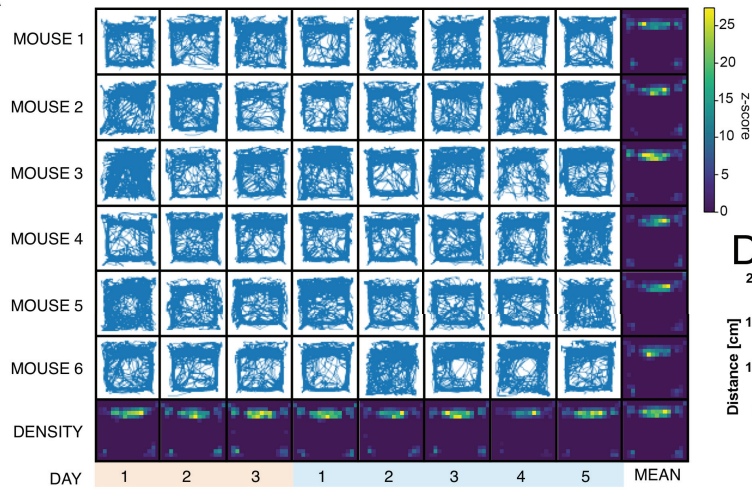
**C**



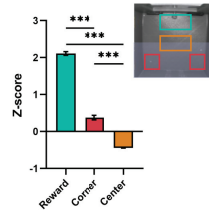
**D**



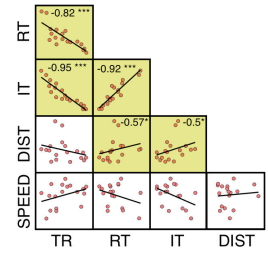
**A**



**B**



**C**



**D**

